

Characterization of Zirconium Cathode Arc-heater Plume by Laser Absorption Spectroscopy

Makoto Matsui*, Tomoyuki Ikemoto†, Hiroki Takayanagi‡, Kimiya Komurasaki§, and Yoshihiro Arakawa**
The University of Tokyo, Tokyo, 133-8656, JAPAN

An arc-heater with pre-mixed gas injection system of argon and oxygen has been developed and its performances were characterized. To reduce the cathode erosion zirconium was used as a cathode material. Consequently, stable discharge was maintained for more than three hours with small cathode erosion rate of 1.7×10^{-5} g/s, which corresponds to the erosion speed of the cathode surface of 0.27 mm/hour. From LAS diagnostics, oxygen was found fully dissociated in the center of plume at the radial position less than 6 mm. The atomic oxygen flux and the total specific enthalpy around the centerline were estimated at 3.1×10^{19} atom/cm²s, 4.5 ± 0.1 MJ/kg, respectively.

I. Introduction

In developing thermal protection systems (TPS) for reentry vehicles, a constrictor-type arc-heater is widely used to simulate such high enthalpy flows because it is simple and rugged structure, long operational time and requires a little maintenance after several-hour operation.^{1,2} Recently, atomic oxygen is found to play important roles through the heat-flux enhancement by catalytic effect and the active-passive oxidation of TPS surfaces.^{3,4}

Atomic oxygen flows are also required to simulate space environments at low earth orbit (LEO). Since spacecrafts have velocities of ~ 7.8 km at LEO, atomic oxygen dissociated by ultraviolet ray from the sun collide with them with a translational energy of ~ 4.5 eV, resulting in the severe degradation of their surface materials.^{5,6}

In the constrictor-type arc-heaters, oxygen is usually injected at the constrictor part to prevent the cathode from oxidation, while inert gas such as argon or nitrogen is supplied from the base of a cathode as shown in Fig. 1. In our previous research, number density distributions of atomic oxygen in argon-oxygen flows generated by constrictor type arc-heaters were evaluated by laser absorption spectroscopy (LAS) and CFD analysis^{7,8} As a result, oxygen was found insufficiently mixed with argon and then little dissociated in the constrictor region. Although the oxygen was gradually mixed in the plume, the dissociation rate was quite small because of the low temperature after nozzle expansion, resulting in the low degree of dissociation in oxygen.

For the enhancement of oxygen dissociation, a hollow cathode arc-heater was developed to supply oxygen through the cathode tip into the high temperature cathode-jet region as shown in Fig.2.⁹ Consequently, the degree of dissociation in oxygen increased. However, the severe cathode erosion up to 1.5×10^{-3} g/s limited the operation time shorter than twenty minute.

Next, we tested the pre-mixed gas injection of oxygen and argon from the base of the cathode. As a cathode material, zirconium was used instead of conventional thoriated-tungsten to reduce the cathode erosion. Zirconium reacts with oxygen and forms an oxide ceramic (zirconia) layer on the cathode surface. This zirconia has the high melting point of 3000 K and lower vapor pressure than oxide tungsten.^{10,11} In this study, the erosion rate of the zirconium cathode was measured, and the degree of dissociation in oxygen and the specific enthalpy was evaluated by LAS.

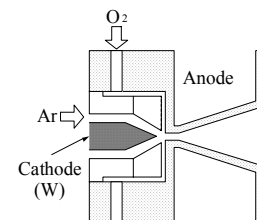


Fig. 1 Conventional injection.

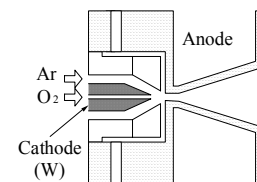


Fig. 2 Hollow injection.

* JSPS Research Fellow, Department of Aeronautics and Astronautics; matsui@al.t.u-tokyo.ac.jp. Member AIAA.

† Graduate student, Department of Advanced Energy.

‡ Graduate student, Department of Aeronautics and Astronautics, Student Member AIAA.

§ Associate Professor, Department of Advanced Energy Member AIAA.

** Professor, Department of Aeronautics and Astronautics Member AIAA.

II. Experimental Method and Apparatus

A. Laser Absorption Spectroscopy

1. Principle of laser absorption spectroscopy^{12, 13}

In LAS, the translational temperature T and the flow velocity u was deduced from an absorption line of ArI at the center wavelength $\lambda_0 = 842.46$ nm.

The relationship between laser intensity $I(\nu)$ and absorption coefficient $k(\nu, x)$ is expressed by the Beer-Lambert law as

$$\frac{dI(\nu)}{dx} = -k(\nu, x)I(\nu). \quad (1)$$

Here, ν is the laser frequency and x is the coordinate in the laser pass direction.

In our experimental conditions, Doppler broadening is several gigahertz, which is two orders of magnitude greater than all other broadenings, including natural, pressure and Stark broadenings. The absorption profile $k(\nu, x)$ is approximated as a Gaussian profile, expressed as

$$k(\nu, x) = \frac{2K(x)}{\Delta\nu_D} \sqrt{\frac{\ln 2}{\pi}} \exp \left[-\ln 2 \left\{ \frac{2(\nu - \nu_0 - \Delta\nu_{\text{shift}})}{\Delta\nu_D} \right\}^2 \right]. \quad (2)$$

Here, ν_0 is the center absorption frequency and $K(x)$ is the integrated absorption coefficient.

$\Delta\nu_D$ is the full width at half maximum of the profile and is related to T , expressed as

$$\Delta\nu_D = 2\nu_0 \sqrt{\frac{2k_B T}{mc^2} \ln 2}, \quad (3)$$

where m , c and k_B represent the mass of absorbers, velocity of light, and the Boltzmann constant, respectively.

$\Delta\nu_{\text{shift}}$ is the shift of center absorption frequency by Doppler effect and expressed as

$$\Delta\nu_{\text{shift}} = \frac{u}{\lambda_0} \sin \theta. \quad (4)$$

Here, θ is the incident angle of probe laser to the flow.

2. Measurement system

A tunable diode-laser with an external cavity was used as the laser oscillator. Its line width was less than 500 kHz. The laser frequency was scanned over the absorption line shape $k(\nu)$. The modulation frequency and width were 1 Hz and 30 GHz, respectively. The laser intensity, which was normalized by saturation intensity, was reduced less than 0.02 by neutral density filters; it was sufficiently small to avoid the influence of absorption saturation. An optical isolator was used to prevent the reflected laser beam from returning into the external cavity. An etalon was used to calibrate relative frequency. Its free spectral range was 0.75 GHz. A glow discharge plasma tube was used as a stationary plasma source to calibrate the laser frequency.

The probe beam was guided to the chamber window through a multimode optical fiber. The fiber output was mounted on a one-dimensional traverse stage to scan the flow in the radial direction. The incident angle of the probe beam to the flow was 75 degree and its diameter was 1 mm at the chamber center. A parabola mirror allowed scanning of the plume without synchronizing the detector position with the probe beam position. Signals were recorded using a digital oscilloscope with 16-bit resolution at the sampling rate of 1 kHz. Figure 3 shows a schematic of the measurement system. A measurement plan was 10 mm downstream of the nozzle exit.

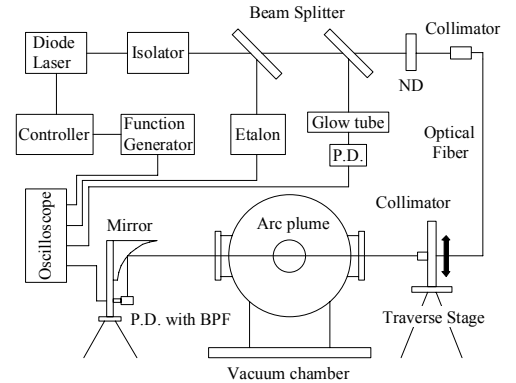


Fig. 3 Measurement system.

B. Zirconium Cathode Arc-heater with Pre-mixed Gas Injection System

The zirconium cathode arc-heater is shown in Fig. 4. Because the thermal conductivity of zirconium is one-tenth of that of tungsten, the length from the cathode tip to the water-cooled copper socket was designed as short as 4 mm, and the tip of the cathode was flattened so as to prevent the cathode from melting. Ahead of the operation, the zirconium cathode was exposed in the arc-heater plume to produce oxide coating for thirty minutes.

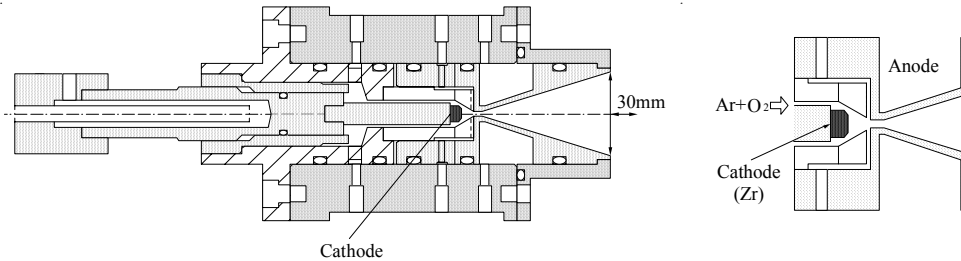


Fig. 4 Schematic of a zirconium cathode arc-heater (left) and pre-mixed injection system (right).

III. Results

A. Cathode erosion

An operation condition is listed in Table 1. A photo in operation of the arc-heater plume is shown in Fig.5. Although the oxide ceramic layer is non-conductive at room temperature, discharge was successfully initiated with a 5 kV high voltage igniter and sustained stably because electric conductivity of the layer increases with the temperature. Figure 6 shows a photo of the zirconium cathode erosion before and after operation. The cathode mass loss was measured after the three-hour continuous operation. As a result, time-averaged erosion rate was estimated at 1.7×10^{-5} g/s, which corresponds to the cathode surface erosion speed of 0.27 mm/hour. When the discharge current was increased to 50 A, the erosion rate was drastically increased as much as 4.1×10^{-4} g/s.

Table 1 Operation condition.

Parameters	Values
Current	40 A
Voltage	27 V
Argon mass flow	4.0 slm
Oxygen mass flow	0.5 slm
Ambient pressure	17.2 Pa
Plenum pressure	22.4 kPa

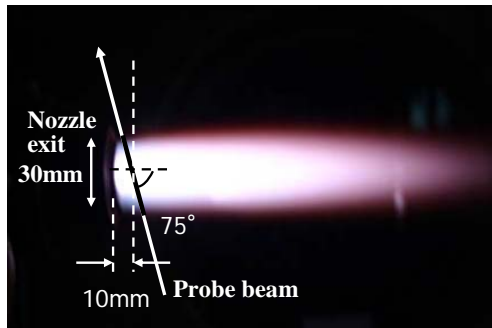


Fig. 5 Photo of the arc-heater plume.



Fig. 6 Erosion of zirconium cathode.

B. Temperature and velocity measurements

Figure 7 shows measured absorption profiles after the Abel inversion. The absorption profiles near the plume centerline exhibit larger absorption and shift than those near the plume edge. T and u were deduced from measured broadening width of the profile and the shift, respectively. Figure 8 shows their distributions along with Mach number $M = u / \sqrt{\gamma RT}$. Here, γ and R are the ratio of specific heat and gas constant, respectively. Although u at the

edge of the plume was subsonic, it might be underestimation because the radial velocity component near the edge would not be negligible.

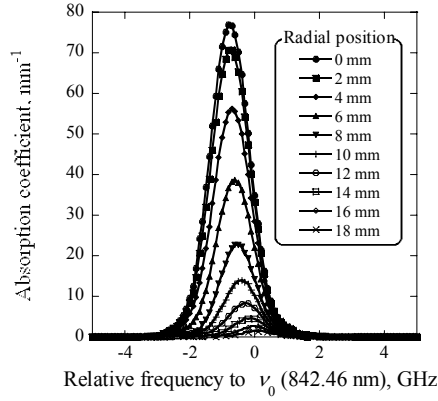
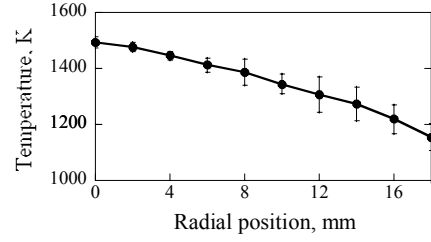
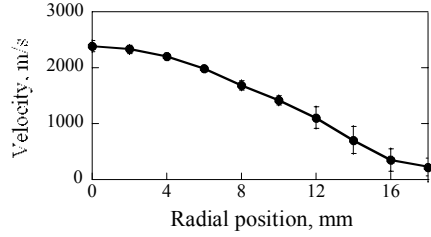


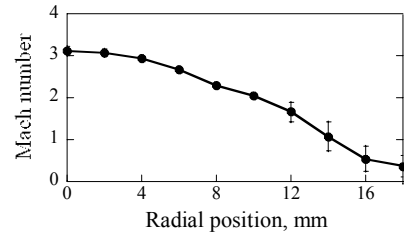
Fig. 7 Measured absorption profiles.



(a) Translational temperature.



(b) Flow velocity.



(c) Mach number.

Fig. 8 Measured flow properties: (a) translational temperature, (b) flow velocity, and (C) Mach number.

IV. Discussion

The specific enthalpy and degree of dissociation in oxygen were estimated as follows. Assuming an isentropic expansion and chemically frozen flow through the nozzle, the total specific enthalpy h_0 is conserved expressed as

$$h_0 = \int_0^{T_0} C_p dT + h_{\text{chemical}} = \int_0^{T_{\text{exit}}} C_p dT + h_{\text{chemical}} + \frac{1}{2}u^2. \quad (5)$$

Here, C_p and T_0 and h_{chem} are the specific heat at constant pressure, the total temperature and the chemical potential, respectively. h_{chem} is constant under the chemically frozen flow assumption.

Since the total pressure p_0 measured in the plenum chamber by a silicon-diaphragm pressure sensor was as high as 22.4 kPa, the chemical composition in the plenum chamber of the flow was calculated assuming thermo-chemical equilibrium. In the calculation, seven chemical species Ar, O₂, O, Ar⁺, O₂⁺, O⁺ and e⁻, and four chemical reactions Ar ↔ Ar⁺+e⁻, O₂ ↔ 2O, O ↔ O⁺+e⁻, 2O ↔ O₂⁺+e⁻ were considered. Their equilibrium constants were obtained from references 12 and 13. The volumetric gas mixture ratio argon and oxygen and p_0 were set identical to the operation condition. C_p was computed as the sum of the contributions of all species. Figure 9 shows the calculated mole fraction and specific enthalpy as a function of T_0 .

Using Eq. (5), T_0 distribution was deduced from measured T , u . It was 6209 K on the axis and 1198 K at the plume edge. Figure 10 shows the distributions of estimated degree of dissociation in oxygen and specific enthalpy. At the radial position $r < 6$ mm, oxygen was fully dissociated. The averaged h_0 at $r < 6$ mm was 4.5 ± 0.1 MJ/kg, in which chemical potential accounted for 32%. Assuming the pressure in the plume was identical to the backpressure in the vacuum chamber, the averaged atomic oxygen flux was estimated 3.1×10^{19} atom/cm²s, and the total plasma power was to be 180 W, which was 17% of the total input power.

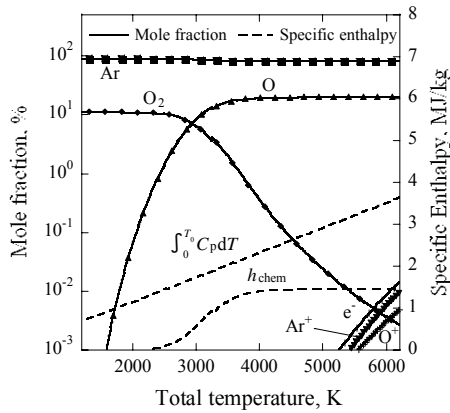


Fig. 9 Calculated specific enthalpy and mole fractions by thermo-chemical equilibrium assumption, $p_0=22.4$ kPa, volumetric mixture ratio Ar: O₂=8:1.

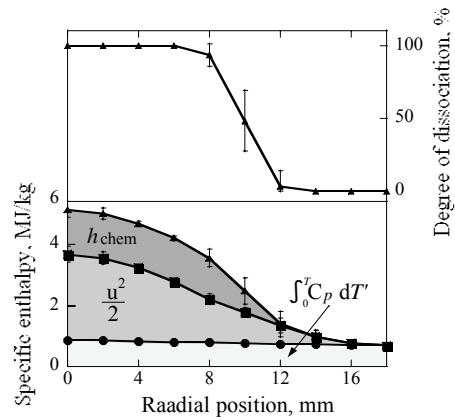


Fig. 10 Degree of dissociation in oxygen and specific enthalpy.

V. Conclusion

Oxygen premixed with argon was supplied from the base of the cathode in the constrictor-type arc-heater. To reduce the cathode erosion zirconium was used as a cathode material. Consequently, stable discharge was maintained for more than three hours with small cathode erosion rate of 1.7×10^{-5} g/s, which corresponds to the erosion speed of the cathode surface of 0.27 mm/hour.

From LAS diagnostics, oxygen was found fully dissociated in the center of plume at the radial position less than 6 mm. The atomic oxygen flux and the total specific enthalpy around the centerline were estimated at 3.1×10^{19} atom/cm²s, 4.5 ± 0.1 MJ/kg, respectively.

Acknowledgments

This research was partially supported by the Ministry of Education, Science, Sports and Culture, Grant-in-Aid for Scientific Research (B), 14350507, 2002 and Research Fellowships of the Japan Society for the Promotion of Science for Young Scientists 16-10857, 18-09885.

References

- ¹Birkan, M. A., "Arcjets and Arc Heaters: An Overview of Research Status and Needs," *Journal of Propulsion and Power*, Vol. 12, No. 6, 1996, pp. 1011–1017.
- ²Auweter-Kurtz, M., Kurtz, H. L., and Laure, S., "Plasma Generators for Re-Entry Simulation," *Journal of Propulsion and Power*, Vol. 12, No. 6, 1996, pp. 1053-1061.
- ³Bykova, N. G., Vasil'evskii, S. A., Gordeev, A. N., Kolesnikov, A. F., Pershin, I. S., and Yakushin, M. I., "Determination of the Effective Probabilities of Catalytic Reactions on the Surfaces on Heat Shield Materials in Dissociated Carbon Dioxide Flows," *Journal of Fluid Dynamics*, Vol. 32, No. 6, 1997, pp. 876-886
- ⁴Balat, M., Flamant, G., Male, G., and Pichelin, G., "Active to Passive Transition in the Oxidation of Silicon Carbide at High Temperature and Low Pressure in Molecular and Atomic Oxygen," *Journal of Materials Science*, Vol. 27 1992, pp. 697-703.
- ⁵Kisa, M., Li, L., Yang, J., Minton, T., Stratton, W. G., Voyles, P., Chen, X., Benthem, K., and Pennycook, S. J., "Homogeneous Silica Formed by the Oxidation of Si(100) in Hyperthermal Atomic Oxygen," *Journal of Spacecraft and Rockets*, Vol. 43, No. 2, 2006, pp.431-435.
- ⁶Fujimoto, L, Satoh, K., Shioya, T., Seki, N., and Fujita, K., "Degradation of Materials by High-Energy Atomic Oxygen," *JSME International Journal, Series A*, Vol. 46, No. 3, 2002, pp.283-289.
- ⁷Matsui, M., Takayanagi, H., Oda, Y., Komurasaki, K., and Arakawa, Y., "Performance of arcjet-type atomic-oxygen generator by laser absorption spectroscopy and CFD analysis," *Vacuum*, Vol. 73, No. 3, 2004, pp. 341-346.
- ⁸Matsui, M., "Application of Laser Absorption Spectroscopy to High Enthalpy Flow Diagnostics," Ph.D. Dissertation, Dept. of Advanced Energy, The University of Tokyo, Mar. 2005.
- ⁹Matsui, M., Satoshi, O., Komurasaki, K., and Arakawa, Y., "Arc-heater as an Atomic Oxygen Generator," AIAA Paper 03-3903, Jun., 2003.
- ¹⁰Marotta, A., "Zirconium cathode erosion rate in a vortex-stabilized air plasma torch," *Journal of Physics D: Applied Physics*, Vol. 27 1994, pp. 49-53.

¹¹Nemchinsky, V. A. and Showalter, M. S., "Cathode erosion in high-current high-pressure arc," *Journal of Physics D: Applied Physics*, Vol. 36 2003, pp. 704-712.

¹²Matsui, M., Komurasaki, K., Herdrich, G., and Auweter-Kurtz, M. "Enthalpy Measurement in Inductively Heated Plasma Generator Flow by Laser Absorption Spectroscopy," *AIAA Journal*, Vol.43, No.9, 2005, pp. 2060-2064.

¹³Demtroeder, W., "*Laser Spectroscopy*," Basic Concepts and Instrumentation, 3rd ed., Springer, Berlin, 2002, pp. 68-72.

¹⁴Matsuzaki, R., "Quasi-One-Dimensional Aerodynamics with Chemical Vibrational and Translational Nonequilibrium," *Transaction of Japan Society for Aeronautical and Space Science*, Vol. 30, No. 90, 1987, pp. 243-258.

¹⁵Guputa, R. N., Yos, J. M., Thompson, R. A., and Lee, K.-P., "A Review of Reaction Rates and Thermodynamic and Transport Properties for an 11-Species Air Model for Chemical and Thermal Nonequilibrium Calculations to 30000K," NASA RP-1232; L-16634; NAS 1.61:1232, 19900801, Aug, 1990.